3.6 A STUDY OF THE SUBCANOPY FLOW KINEMATICS IN TWO FORESTS

Ralf M. Staebler[1*] and David R. Fitzjarrald[2]
[1]Meteorological Service of Canada, Toronto, ON
[2]Atmospheric Sciences Research Center, Albany, NY

1. INTRODUCTION

A better understanding of the kinematics and dynamics of subcanopy flows is desperately needed to evaluate their role in the transport of scalars, particularly in complex terrain. Applications of the results range from understanding horizontal transport of CO_2 (Staebler and Fitzjarrald, 2004a) to the dispersion of pollen and spores and the investigation of disease vectors in forest canopies (Moore, 1987; Aylor, 1999). We still do not clearly know the characteristic scales in subcanopy motions, and therefore we do not have a clear understanding how to model them.

Most previous studies have focussed on the downward mixing of momentum into the canopy. In this study, we consider the more complex realities where this feature is joined by other momentum sources and sinks. An essential part of explaining the observations is a detailed description of the canopy structure in both vertical and horizontal dimensions. Both the canopy structure and the local topography are important influences that can produce significant forcing terms in the momentum equation, through drag, buoyancy and pressure effects.

The assumptions of horizontal homogeneity generally applied by those making flux measurements over forests are often violated in the real world to a degree that could produce significant errors (e.g. Baldocchi et al., 2001). Little research has been published on the kinematics of subcanopy flows in forests. Wilson et al. (2001) studied the spatial coherence of CO_2 fluxes using 3 sonic anemometers alternately separated horizontally or vertically in the subcanopy, but made no reference to the mean wind field. A study of advection of CO_2 in Belgium showed evidence of drainage flows on what was assumed to be a 2-dimensional forested slope, but did not provide any additional information on wind fields (Aubinet et al., 2003).

Neither of these studies was primarily concerned with subcanopy kinematics or addressed questions of dynamic forcing. They were limited to relatively short periods (less than a season) or relatively small spatial extent (25 m in Wilson et al. (2001), 50 m in Aubinet et al., 2003). In all cases relatively homogeneous terrains were selected to simplify interpretation. In contrast, the study presented here spans four years, three seasons and an area of 80 m by 80 m around an active AmeriFlux tower site (Harvard Forest), in relatively complex terrain typical of much of the Earth's surface.

Corresponding author address:
Ralf M. Staebler
Meteorological Service of Canada
4905 Dufferin St., Toronto, ON M3H 5T4
ralf.staebler@ec.gc.ca

To contrast the results with those obtained in simpler terrain, a smaller, comparative study was conducted at a ecologically similar, but topographically different site, at the Borden Forest Research Station.

This paper does not provide a comprehensive description of all aspects of subcanopy flows – clearly an unrealistic ambition. However, several methodologies, developed in the course of this study, are described that will be of interest to those in search of a better understanding of subcanopy structure and kinematics.

2. THEORY

The slope momentum equation describes flows both above and below the canopy:

$$\frac{\partial u_i}{\partial t} + u_j \frac{\partial u_i}{\partial x_j} = \underbrace{-\frac{\partial \tau_{ij}}{\partial x_j}}_{[1]} + \underbrace{g \frac{\theta_v^*}{\overline{\theta_v}} \frac{\partial h}{\partial x_i}}_{[2]} \underbrace{-\frac{1}{\rho} \frac{\partial p}{\partial x_i}}_{[3]} + \underbrace{F_{D,i}}_{[4]} \quad (1)$$

where h represents the topographic elevation, τ is the stress tensor, $\overline{\theta_v}$ is the mean virtual potential air temperature and θ_v^* the local departure from it. The right-handed coordinate system is defined by i=1 being parallel to the slope and i=3 perpendicular. A repeated index indicates summation. Term [3] describes the horizontal pressure gradient, while $F_{D,i}$ represents the sum of all drag forces, and is zero above the canopy. The Boussinesq approximation has been applied, and the rotation of the Earth and molecular dissipation neglected.

Reynolds stress divergence [1] results from coupling with the flows aloft. The degree of vertical coupling of momentum into the canopy strongly depends on the canopy density. In forests with high leaf area indices, subcanopy flows are often effectively decoupled, especially at night (Fitzjarrald and Moore, 1995). In other words, momentum transfer into the subcanopy may often be insignificant relative to the generation of momentum through other mechanisms.

Term [2] describes the forcing generated when radiative cooling near the ground creates negative buoyancy, which will cause the colder air to flow downhill. Here it is important to differentiate between drainage flow and katabatic flow. Term [2] describes katabatic flow because the forcing is local, i.e. both slope and temperature inversions apply to the locally measured layer. Drainage flow, on the other hand, can describe a

flow for which the negative buoyancy was generated some distance from the point of interest, through the same processes, but is advected to the point of interest through the momentum advection term $u_j \frac{\partial u_i}{\partial x_j}$ (cf. Fitzjarrald, 1984). Determining the direction from which these buoyancy flows will emanate is generally not obvious in complex terrain, and different scales can affect the local flow under different conditions (Mahrt et al., 2001).

The theory of drainage flows for simple geometries has been discussed comprehensively in the literature (cf. Prandtl, 1942; Fleagle, 1950; Mahrt, 1982; Fitzjarrald, 1984). Equilibrium between advection of momentum along the slope and the vertical stress divergence, as well as between horizontal heat advection and vertical heat divergence, yields the classical steady katabatic, nose-shaped wind profile. To date, there is little information in the published literature on the depth of drainage flows inside canopies, where the situation is complicated by the unknown frictional effects of the array of trunks present. The simplest parameterization with constant eddy diffusivity (e.g. Prandtl, 1942) is probably not applicable there, but appropriate models have yet to be established and tested. Moreover, characteristic scales needed to specify the eddy diffusivity, as for 2nd order closure models (e.g. Poggi et al., 2004) or large eddy simulations (e.g. Fitzmaurice et al., 2004), have not been observationally validated to date. Most previous studies have concentrated on neutral conditions, with little modeling of light wind conditions typical of the nocturnal subcanopy.

Term [3] (pressure perturbation) is also potentially important, especially in the lee of hills. Only recently have modeling and wind tunnel studies of canopies on hills become available. Finnigan and Belcher (2004) used a linear hill flow model based on Hunt et al. (1988), which they modified by covering the hill with a homogeneous canopy. The results for steady-state conditions under neutral stratification indicate a region of reversed flow on the lee side. In the upper canopy, there is an approximate balance between the pressure gradient perturbation and the vertical transport of momentum, while, deeper in the canopy, the pressure gradient perturbation balances the drag forces. By balancing the pressure forcing term with the stress divergence, a level in the canopy on the lee side of a ridge can be estimated where the wind speed drops to zero. If the canopy is deeper than this level, flow separation and a region of reversed flow should be expected. This level is estimated to be about 10 m at the Harvard Forest, and since the canopy has a depth of about 20 m, there should be flow reversal in the bottom half.

Upon generation, these subcanopy flows are then modified by the immediate local topography and by obstacle effects (e.g. the vegetation). The drag force (term [4]) is generally parameterized as $\vec{F}_D = -(C_D)(CAD)|\vec{u}|\vec{u}$, where C_D represents a drag coefficient, *CAD* is the canopy area density, and the product of the wind vector with its absolute value ensures that the drag force opposes the flow (cf. Kaimal and Finnigan, 1994, p.95).

To understand the flows in and above a forest in complex terrain, detailed measurements were conducted at the Harvard Forest using sonic anemometers at several levels from the ground up to 29m and an acoustic sounder to measure winds aloft. These data are contrasted with similar data obtained at a topographically distinct, yet ecologically similar forest. The data collected in these studies represent the most comprehensive set of subcanopy flow observations covering a time frame of several months to date, and provide additional insights into subcanopy dynamics. While these measurements still fall short of completely describing subcanopy flows, they allow the testing of some hypotheses regarding their driving mechanisms.

3. SITES AND METHODS

Data from two sites are described in this paper: the Harvard Forest (Petersham, MA, 42°32'N, 72°11'W, 340m ASL), and the Borden Forest Research Station, operated by the Meteorological Service of Canada (CFB Borden, 44°19'N, 79°56'W, 215m ASL).

To monitor the wind speeds in the subcanopy at the Harvard Forest, a network of sonic anemometers was deployed in a grid of 80 m by 80 m, 1.8 m above the ground (Figure 1). A 5 m tower at the center of the grid was instrumented for detailed profiles of temperature, humidity and CO_2 to supplement the profiles on the main flux tower, 11 m to the south. SPAS/2Y 2-axis sonic anemometers (Applied Technologies, Inc.) with a resolution of 0.01 m s^{-1} were used on the periphery of the grid, and a Gill HS (Gill Instruments Ltd.) 3-axis sonic anemometer operated at the center of the grid. In the vertical, 3-axis sonic anemometer data was available at 29 m, 17 m and 8 m (SATI, Applied Technologies, Inc.) on the main tower, and at 5 m and 3 m on the 5 m tower (CATI/2, Applied Technologies, Inc.). Details on the continuous measurements at the Harvard Forest, as well as on the subcanopy measurements, can be found elsewhere (Moore et al., 1996, for the former; Staebler and Fitzjarrald (2004a, b) and for the latter, Staebler (2003).

Vertical profiles of the canopy area density (*CAD*) were obtained using the methods of Parker et al. (2004b), by walking six parallel transects through the forest, covering the aforementioned grid, with an upward-looking laser range finder (LD90-3100HS, Riegl Laser Measurement Systems GmbH, Horn, Austria). This method is complementary to use of an airborne, downward-looking instrument being developed to map topography and vegetation from a satellite platform (Blair et al., 1999).

To relate the horizontal obstruction effects experienced by the flow field to the physical obstacles, the same laser was used to obtain horizontal scans. A turntable mounted on a tripod was designed, on which the laser was mounted in addition to an electronic compass (EZ Compass 3, Advanced Orientation Systems, Inc.,

Linden, NJ) to keep track of the direction in which the laser was pointing.
Measurements of the wind fields up to levels of typically 500 m above ground were conducted at both sites with Doppler sodar instruments (REMTECH PA-1, France). This instrument provides 30 levels of echo strengths (related to the local temperature structure function C_T^2, a measure of the amplitude of temperature fluctuations in the air), wind speeds and directions, as well as derived quantities such as the Reynolds stress tensor and an estimate of the inversion or mixing height. The manufacturer claims vertical and horizontal wind speed accuracies of 0.05 m s^{-1} and 0.2 m s^{-1} respectively, and a directional accuracy of 3°.

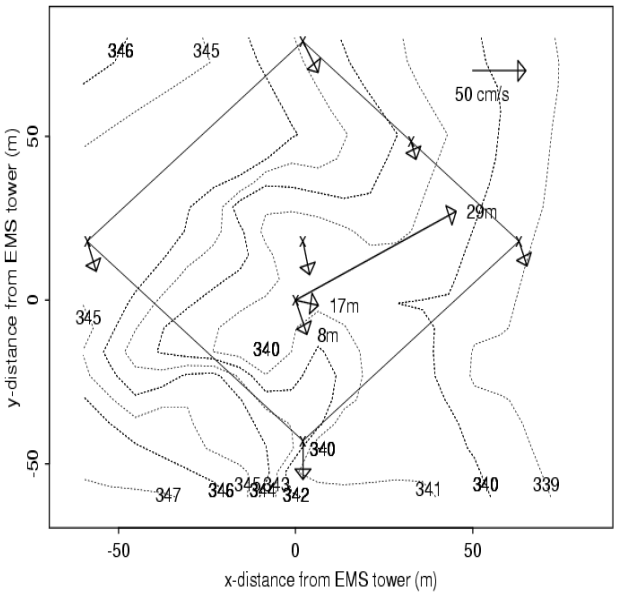

Figure 1. Locations of the anemometers for the studies at the Harvard Forest in 2001 and 2002, marked by "X" symbols and wind vectors. A 3-minute average wind field (10 Sept 2001, 7:20 EDT) is shown as an example. The main tower anemometers are identified by wind vectors with labels indicating the height of the anemometer (8, 17, 29m). Dotted lines denote local topography in *m ASL*.

Information on the continuous measurement program at Borden can be found in Staebler et al. (2000). To monitor the understory flows, a Kaijo-Denki 3D sonic anemometer (model TR-90AH) was installed in June 1999 at 1.4m above ground; a second one was added in July 2000, and a third (CSAT, Campbell Scientific Inc.) in July 2001, within a radius of 54 m of the main tower.

4. OBSERVATIONS

4.1. THE PHYSICAL STRUCTURE OF THE CANOPY

Data to investigate the effects of canopy structure and topography on the flow fields above and within a forest were obtained at both the Harvard Forest and Borden. One expects that the more complex terrain and the larger slopes at the Harvard Forest could support drainage flows from several potential airsheds. Slopes at Borden are much smaller (less than 10m/km), but not insignificant.
To quantify the obstacle effect on the subcanopy wind measurements, the empirical concept of "transmission factors" (Fujita and Wakimoto, 1982) was applied to each of the subcanopy anemometers (Figure 1). Winds were binned into 30° wind direction sectors, and the average wind speed for each sector for each anemometer was calculated. The maximum wind speed in the network for this sector was then defined to be the reference (relatively unobstructed) wind speed, and the ratio of the wind speed of each anemometer to this reference was called the transmission factor (*TF*), i.e.

$$u(\phi,\vec{x}) = TF(\phi,\vec{x})U(\phi) \qquad (2)$$

where *u* is the wind speed for wind direction ϕ at location $\vec{x}$ and *U* is the network reference. To obtain a hypothetical wind field unaffected by these localized differences, winds can then be corrected for the obstruction effect by dividing by the appropriate *TF*.
To relate the size of obstacles to a transmission factor, Fujita and Wakimoto (1982) stated that only the angular size of the object was of importance, and expressed $TF = e^{-k\phi}$, where ϕ is the vertical angular size of an obstacle and *k* is an empirically determined coefficient. In a follow-up paper (Wolfson and Fujita, 1989), they included a constant; also, they stated that this only works for a certain range of wind speeds and that it would help to parameterize the wind speed dependence.
The approach using vertical angular sizes of obstacles is not applicable inside a forest. Instead, we apply horizontal angular sizes, weighted by distance to the obstacles. Inside this type of forest, every direction is obstructed within less than 50 m. Since it is reasonable to assume that nearer objects should be weighted more heavily, and since the angular size of any object is given by *d/r* (where *d* is the width of the object, e.g. the diameter of a trunk, and *r* the distance), the approach taken was to add the inverse of the laser distances *r* (which are all equally spaced in direction θ) for a given sector to give an obstruction parameter,

$$N_{\Delta\theta} = \sum_{\Delta\theta} 1/r \qquad (3)$$

To convert this obstruction parameter to a pseudo-TF, we calculate

$$TF'(\Delta\theta) = 1 - \frac{N(\Delta\theta)}{N_{\max}(\Delta\theta)}, \qquad (4)$$

where N_{max} is the maximum obstruction parameter found in the network in sector $(\Delta\theta)$. These TF values

were then normalized relative to their maximum and smoothed with a 90° symmetric triangular filter (Figure 2).

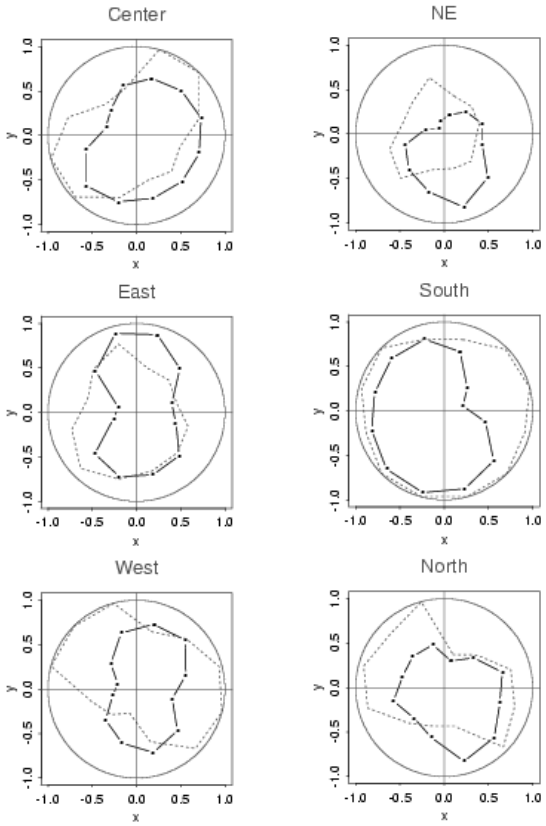

Figure 2: Wind-derived (dashed) and laser-derived (connected dots) transmission factors for spring 2002. Headers refer to anemometer locations (see Fig. 1).

The effect of wind speed on the obstacle effects was tested by re-calculating the wind-based transmission factors for wind speeds above and below 0.2 m s^{-1} (the subcanopy median). The higher wind speeds generally resulted in better agreement between the two methods. Higher wind speeds consistently show up best at the South site, which therefore automatically acts as the reference site.

In close proximity to obstacles, the transmission factor cannot tell the whole story. Some measure is required of the deflection of the flow around the obstacles. Significant and systematic deflections are observed at the different sites. A small part of these deflections is due to flow distortion by the instruments themselves (Kaimal et al., 1990), but this was found to be typically less than 5° during the cross-comparison period when all instruments were collocated. Most of the deflection is therefore due to understory obstacle effects. Given typical wind speeds of 0.2 m s^{-1} and trunk diameters of 0.1 m (i.e. Reynolds number Re ≈ 1500 for kinematic viscosity $\upsilon \approx 1.5 \times 10^{-5}$ m^2 s^{-1}), laminar flow is still plausible in many cases. Deflection angles would be expected to peak on the sides of the largest obstruction densities (lowest transmission factor), i.e. line up with the maximum rate of change of the transmission factor. There is some evidence of this in the data (Staebler and Fitzjarrald, 2004b).

4.2. SUBCANOPY METEOROLOGY AT THE HARVARD FOREST

Median profiles of temperature and wind speed (Figures 3 and 4) indicate that stable stratification is the norm in the bottom 8 m of this forest except during leafless periods with bare ground, when a combination of the soil's thermal inertia and direct insolation keep the ground warmer than the air above it. The daytime profiles during summer indicate radiative warming of the foliated canopy space while the lack of sunlight reaching the floor (typically < 10%) results in colder air near the ground. The nocturnal profile in the summer also clearly shows the effect of the foliage in preventing mixing with the air aloft, with the temperature approaching the above-canopy value more slowly than in winter. In summary, conditions for negative buoyancy near the ground, conducive to drainage flows, exist 83% of the time (92% of the time at night, 65% during daytime). To determine the behavior of the subcanopy flow, the relative sizes of the other forcing terms have to be considered as well.

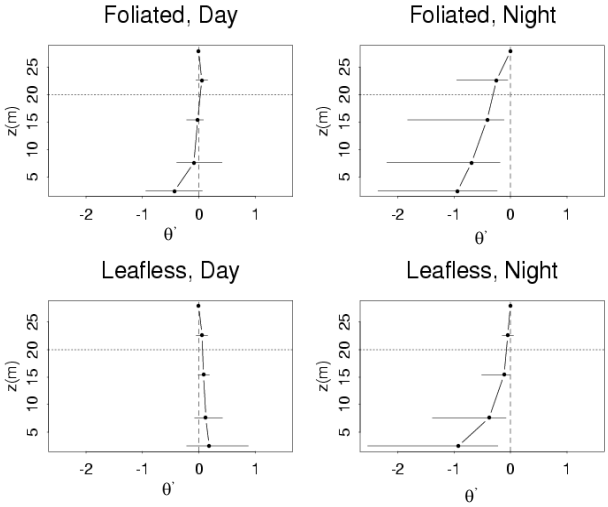

Figure 3. Median potential temperature profiles at the Harvard Forest for over 12000 half-hours from 1999-2002. θ' represents the difference (in degrees Kelvin) to the temperature at 30 m. The horizontal bars denote the interquartile range. The foliated period corresponds to DOY 160-260, the leafless period to DOY 1-120 and 300-365. Day is defined as 9:00-17:00 EST, night as 20:00-4:00 EST.

The wind speed profiles (Figure 4) display exponential behavior inside the canopy, as parameterized by Cionco (1985), only in the leafless state, when the *CAD* profile is relatively straight (see below). During foliated periods, the wind speed increases only by about 60% from 1.8 m to the top of the canopy, compared to a factor of more

than 3 in winter. The ratio of the wind speed at 1.8 m to the wind speed at 29 m stays almost constant throughout the year. The foliated profiles also indicate the difficulties of making representative wind speed measurements inside a canopy: the lower values of the wind speed at 20 m are due to a slightly greater proximity of canopy elements to the tower at this level, as verified during the transects described in 3.2. Clearly, the Cionco (1985) approach only applies to horizontally and vertically simple canopy structures.

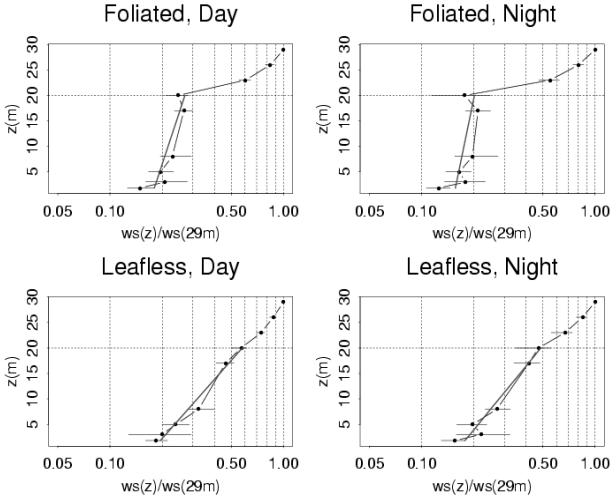

Figure 4. Similar to Figure 3 for the profiles of wind speeds relative to the wind speed at 29m. The points at 26 m, 23 m and 20 m represent cup anemometer data (2nd, 3rd and 4th from the top), while the rest are based on sonic anemometers. The straight lines represent exponential fits to the wind profile below 20 m.

4.3. SUBCANOPY FLOWS

Subcanopy flows are generated through a balance of four driving forces (Equation 1): pressure gradient perturbations, buoyancy, stress divergence, and canopy drag. Since drag effects will not have a large effect on directionality of the flow on the same scale as the three driving forces, but only in very close proximity to obstacles, it is ignored in the subsequent analysis. The transmission factors projected and measured in section 4.1 are local manifestations of drag in the immediate surroundings of the anemometers, and these have been taken into consideration (see below).

In over 12000 half-hour averages collected during the studies from 2000-2002, only 25% show alignment between the wind vector at 29 m and at 1.8 m within an angle of ± 30°. The fractions for alignment within ± 30° between the 3D anemometer at 1.8 m and other anemometers horizontally displaced by 40-60 m are typically around 60%, while the wind vectors directly above the 3D anemometer at 3 m and 5 m were aligned to this degree 76% and 72% of the time respectively. Those at 8 m and 17 m on the main tower nearby are aligned with the 1.8 m wind vectors 30% and 27% of the time, respectively. This makes it clear that the airflow in the subcanopy is frequently not driven simply by momentum transfer from aloft.

To determine the relative importance of the three driving forces on the flow near the ground, they were parameterized as follows. The stress term was taken to be the vertical gradient of the momentum flux between 8.2 m and the ground (where it goes to zero). The buoyancy term was calculated using the potential temperature at 2.5 m minus the average temperature between 15 and 28 m. A representative 4.5° topographic slope was used.

Estimating the pressure gradient term involved some assumptions. The linear theory by Hunt et al. (1988) as described in Finnigan and Belcher (2004) predicts a maximum pressure gradient for a series of sinusoidal 2D hills to occur halfway downhill in the lee of the peak and to have a maximum magnitude of $\frac{\partial p}{\partial x} \sim \rho U_0^2 \frac{H}{2} (\frac{\pi}{2L})^2$, where U_0 is a reference wind speed inside the "middle layer" (which is rotational but not affected by turbulence near the ground), estimated to be around 800 m above ground given the topography at the Harvard Forest. This wind speed was extrapolated from measurements at 30 m using a relationship established from periods of measurements at both levels (the 800 m data deriving from radar wind profiler measurements 9.5 km to the WNW (courtesy of NOAA). *H* and *L* were determined from topographical maps, and were allowed to vary according to wind direction. The fractions to be used in the following analysis can then be summarized thus:

$$t_a = \left| \frac{\partial \tau}{\partial z} \right|$$
$$p_a = \left| \frac{1}{\rho} \frac{\partial p}{\partial x} \right|$$
$$b_a = \left| g \frac{\theta_v^*}{\theta_v} \frac{\partial h}{\partial x} \right| \qquad (5)$$

and

$$tfrac = t_a / (t_a + p_a + b_a)$$
$$pfrac = p_a / (t_a + p_a + b_a)$$
$$bfrac = b_a / (t_a + p_a + b_a)$$

As expected, these calculations suggest a stronger role played by stress divergence during the day, and buoyancy at night (Figure 5). The pressure term, which is based on the assumptions referenced above and may well be overestimated, appears relatively invariant, but is as significant as the other two terms. On average, the *bfrac* is 52% (26%), *pfrac* 33% (35%), and *tfrac* 15% (38%) during the night (day).

Analysis of the seasonal cycle of these forcing terms showed that the stress divergence term appears most significant in the subcanopy during daytime in late

winter / early spring and then again in the fall (Figure 6). These are periods when the forest is leafless and momentum can penetrate more easily through the canopy. A secondary minimum in the winter is due to the seasonal variation in synoptic wind speeds, diminished in winter because of the frequent occurrence of stable systems with smaller synoptic pressure gradients. Nights are dominated by buoyant forcing throughout the year, but especially so during the spring when the temperature gradients close to the ground are strongest because of the cold ground and the warming air aloft. The fraction of nights with $u_* < 0.2$ m s^{-1} is almost constant throughout the year, ranging from a minimum of 29% in May to a maximum of 34% in July.

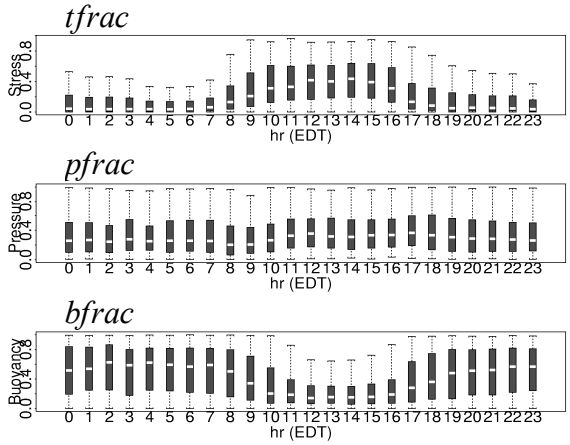

Figure 5. diurnal cycle of stress divergence, pressure gradient and buoyant forcing fractions (*tfrac, pfrac* and *bfrac),* for all Harvard Forest data, 1999-2002. The interquartile range is given by the box, the median by the white line in it, and the outliers by the whiskers.

To determine the effect of these different forces on the subcanopy flow, different flow characteristics must be isolated. Flows generated by the buoyancy term are expected to come from the direction of the dominant slope, although it is not obvious at the Harvard Forest what this may be. To see whether there is a preferred subcanopy wind direction under strongly buoyant conditions, wind roses were plotted for increasing fractions of the buoyant term (Figure 7). These show that NW and N flows increase as negative buoyancy becomes dominant. On average, 37% of all subcanopy winds come from the NW when *bfrac* >80% and 25% from N, compared to 13% and 22% respectively when *bfrac* < 20%. This trend is consistent from year to year and applies at all points in the anemometer network. Averaged over all nights, 51% of flows came from wind directions between 300^o and 30^o.

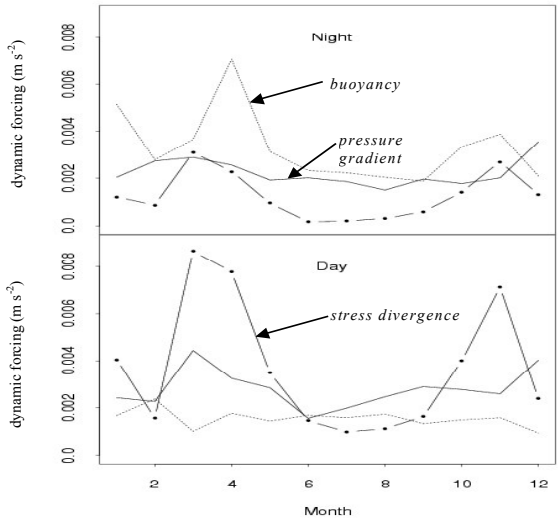

Figure 6. Seasonal cycle of the subcanopy flow forcing terms, at the Harvard Forest. Connected dots: stress divergence term; dotted line: buoyant term; solid line: pressure gradient term.

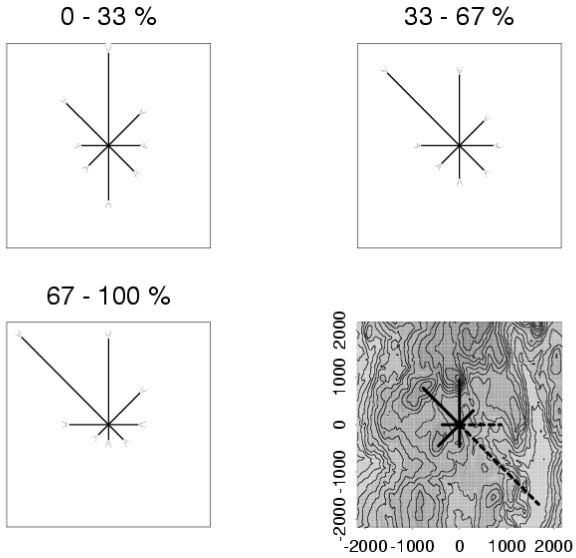

Figure 7. Wind roses as a function of the fraction of the buoyant term in the sum of the forces, based on statistics for all data (8700 half-hours). The final panel shows a topographic map centered at the Harvard Forest flux tower. The solid (dashed) radials indicate the distance to the nearest hilltop (valley), i.e. the nearest significant topographic inflection point. The horizontal scale is in [m], and the contour spacing is 16 m. [Reprinted from Agricultural and Forest Meteorology, Vol.122 No.4**,** Staebler and Fitzjarrald, "Observing subcanopy CO2 advection", 139-156, Copyright (2004)].

Rather than the topography in the immediate vicinity of the tower, which slopes down towards to NE, or the steepness of the most significant slopes within a few km, the deciding factor on the direction of drainage flows appears to be the combined length of uphill plus downhill slope along an axis. This argument is strengthened by results at Borden (section 4.5). Physically this can be explained by the continuous addition of momentum to the flow over a longer distance, if the air close to the ground continues to be cooled.

If the predictions in Finnigan and Belcher (2004) apply to the slopes at the Harvard Forest, there should be observable flow reversals near the ground when a sufficiently strong wind aloft flows over the elevated ground to the west and north before reaching the tower site. Cases with low buoyant forcing (<10%) were separated out and split by the fraction of the pressure gradient term (Figure 8). There was some indication that the relative fraction of reversed flows increases as the pressure gradient fraction increases. However, there was no clear separation between alignment (stress dominated) and reversals (pressure dominated), and the whole spectrum of angles was observed, even at the extremes when the angles should have congregated either near 0^o or 180^o. The linear theory also predicts a speed-up of the flow aloft, due to the Bernoulli effect, of about 100% at heights of about 150 above ground for this topography. Combining local sodar wind profile measurements with radar profiler measurements 10 km to the WNW suggested a speed-up of 20-60% at heights, which is significantly less than predicted.

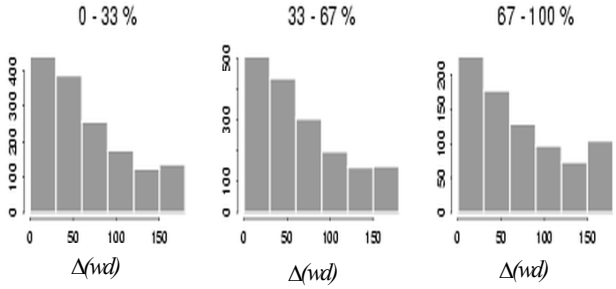

Figure 8. Histograms (number of occurrence, for half-hourly averages with buoyant forcing fractions < 10%) of the angle between the wind directions at 29m and at 1.8m ($\Delta(wd) = |wd(29m) - wd(1.8m)|$) as a function of the pressure gradient fraction.

Attempts to construct the subcanopy wind vector through vector addition of the predicted components (with the buoyant term vector fixed to the longest slope and the stress divergence and pressure gradient vectors aligned with or opposing the wind aloft, respectively) met with limited success, except during drainage flow conditions.

4.4. SUBCANOPY FLOW DIVERGENCE

To research the kinematics of subcanopy flows, a horizontal network must be deployed, usually with limited resources. In this section we focus on two questions: a) can we measure the flow divergence with a small network of sonic anemometers?, and b) is the divergence constant with height, thus allowing for measurements at a single level? The continuity equation for incompressible flow gives

$$\int_0^h (\nabla_{hor} \cdot \vec{u}) dz = -\overline{w}(h) \qquad (6)$$

Lee (1998) and Finnigan (1999) asserted that $\frac{\partial \overline{w}}{\partial z} = \frac{\overline{w}_h}{h}$, i.e. that $\overline{w}$ increases linearly with height, even in the subcanopy, such that $h(\nabla_{hor} \cdot \vec{u}) = -\overline{w}(h)$. This assertion is tested with data from the Harvard Forest.

The uncertainty in the divergence measurement comprises instrumental, random (meteorological) and systematic, obstacle-related components. The instrumental uncertainty was estimated by co-locating all sonic anemometers horizontally within 4 m of each other, and calculating the divergences that would appear in our network with such signals. This component includes errors due to instrumental interference with the wind (e.g. transducer shadowing effects). An 8-day co-located run produced what would be an average divergence of (4 ± 2) x 10^{-5} s^{-1} for the actual network, i.e. well below measured divergences (see below).

These calculations indicate that the measurement of divergence is not limited by instrumental uncertainties. To see whether the flow deflections at each subcanopy site played a significant role in the calculated divergence, wind vectors were corrected for these deflections (section 4.1) and the divergence recalculated. No systematic difference was found between these two sets of divergences, but the noise on the corrected divergences (variance from half-hour to half-hour) was significantly increased (by about 30%). Applying this correction did not improve the correlation between divergences and vertical mass flow (see below).

To test the consistency of the data and whether the divergence is constant with height, one relates the divergences to the vertical mass flow. After removal of the directional dependence (i.e. the streamline component) of $\overline{w}$ using the technique of Lee (1998), the vertical velocities at 29, 17 and 8 m were compared to the divergence in the subcanopy. As an example, we examine an 8-day period in 2001 with an unusually pronounced diurnal cycle in the divergence (Figure 9). While $\overline{w}$ *(8 m)* appears anti-correlated with the divergence on days 317, 318, 319, 322 and 322, and has the correct magnitude, the relationship breaks down on the other days. No correlation is observed with the anemometers at 17 m and 29 m except on day 322. Signals at 5 m and 1.8 m are difficult to interpret, most likely because mean vertical components at these levels approach the instrumental limits.

In the 10-day period shown, the correlation between the divergence and $\overline{w}$ *(8m)* suggests that the assertion of constant divergence with height may hold up to 8 m, but that vertical mean motions above this are decoupled (except on DOY 322, when there is some sign of correlation all the way to 29m). However, this period does not represent the norm. Just as often, the divergence is positively correlated with $\overline{w}$ at the various levels, which can only be explained by the flows below 1.8 m being decoupled from those above. The most consistent pattern observed was that all periods with persistent subcanopy flows from 90° to 180° were associated with positive divergence. This may be due to the local topography. From these directions, deflection of the flow along the topographic contour lines results in an increased divergence.

Plotting the divergence measured at 1.8 m versus the measured vertical velocity shows a lack of any clear correlation. A better correlation can be found when vertical velocities at the various levels are compared, with r^2 = 0.27 and 0.14 for the fits of $\overline{w}$ at 17 m and 8 m against $\overline{w}$ at 29 m, respectively. However, the slopes for the least squares fit (0.45 ± 0.02 (mean ± s.e.) and 0.23 ± 0.01 respectively) were somewhat less than the ratios of the heights (17/29 and 8/29), which means that $(h)(\nabla_{hor}\cdot\vec{u})=-\overline{w}(h)$ may be an oversimplification, or that the divergence may increase with height. Given the scatter on the relationship, however, the assertion of linear increase of $\overline{w}$ with height cannot be statistically disproved.

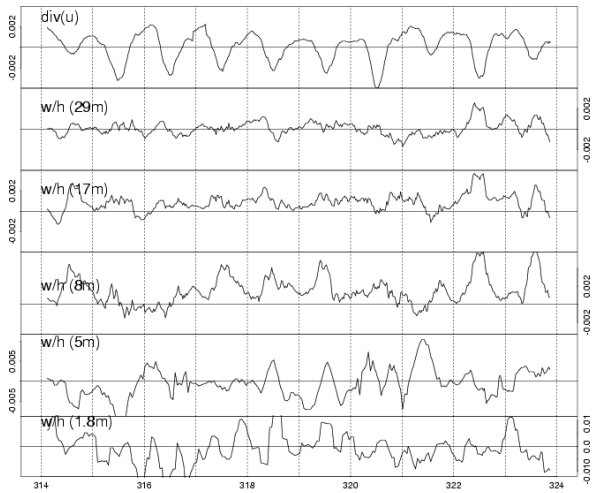

Figure 9. The horizontal divergence at 1.8 m in comparison with $\overline{w}/h$ at all available levels, for a 10 day period in November 2001 (Day of Year 314-324). Shown are half-hour means, smoothened with a 6-hour running mean. All values are in s^{-1}.

While this discussion sheds some light on subcanopy kinetics, the measurements do not suffice to provide a comprehensive picture. Given the complexities of the vertical and horizontal distribution of canopy elements, the possibility of persistent mid-canopy circulations cannot be excluded. In response to the first question posed, it appears that measuring the subcanopy divergence is not limited by instrumental capabilities, but the consistency of the measured divergences could not be confirmed through comparison with the mean vertical velocities. In response to the second question, our results suggest that divergence at this site is not constant with height, although this possibility cannot be excluded statistically. For future field studies, we recommend measuring the divergences at several vertical levels and on varying horizontal scales, which could be done with a network of canopy towers, instrumented at several key levels.

4.5. COMPARISON TO BORDEN

The topography at Borden does not include any large slopes that would at first sight suggest the development of sustained slope flows. The dominant meso-scale signature at Borden is the lake-breeze effect due to the Georgian Bay, 20 km to the northwest.

As at the Harvard Forest, temperature profiles at Borden (Figure 10) are stable in most cases except during daytime in the winter, when solar radiation can penetrate easily to the ground. This may be conducive to gravity flows, although the local slopes are relatively small.

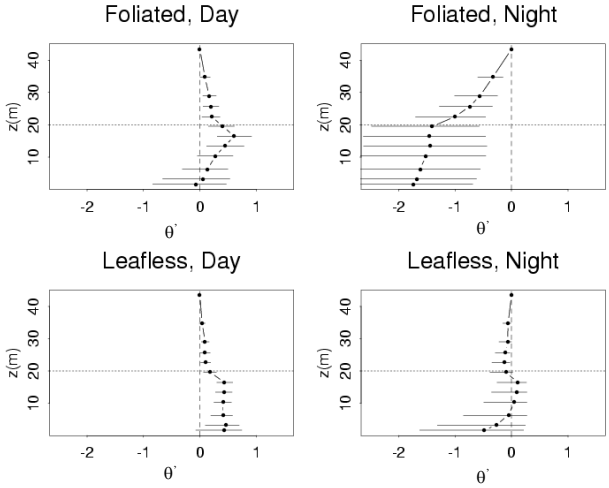

Figure 10. Potential temperature profiles for Borden, 2002, similar to Figure 6 for the Harvard Forest.

Borden was initially meant to serve as a control site at which subcanopy flows would be well correlated with the wind aloft due to the relatively flat terrain. However, measurements quickly showed that even there the subcanopy flows were usually decoupled. A strong dominance of flows from the south and south-west was evident. This coincides with a small (0.3°) but steady slope extending from 1.5 km at SSW to more than 4 km at NNW (Figure 11).

The dynamic forcing components were calculated as described in Equation (5), except that no topographic pressure forcing term was included. Flows aloft are predominantly from the NW at Borden. In the subcanopy, flows from the S and SSW dominate the wind roses (Figure 11) even when the buoyant fraction is small (69% of the time), but increases even more (to 88%) as the buoyant fraction becomes dominant. As at the Harvard Forest, it is not the steepest slope which produces local drainage flows, but the slope with the largest horizontal extent.

On average, subcanopy flows are aligned with flows aloft to better than 30^o only 24% of the time. For wind directions aloft between 90^o and 270^o, the fraction is 39%, and for the northern sector (270^o and 90^o) 7%, while for this sector the flows oppose each other within ($180^o \pm 30^o$) 28% of the time. The de-coupling of the subcanopy flows from the flow aloft appears even more complete at Borden than at the Harvard Forest. The best explanation for this is Borden's higher CAD and more evenly distributed upper canopy. Therefore even at Borden, considered one of the flattest AmeriFlux sites, subcanopy flows are generally driven through forces other than simple downward transport of momentum.

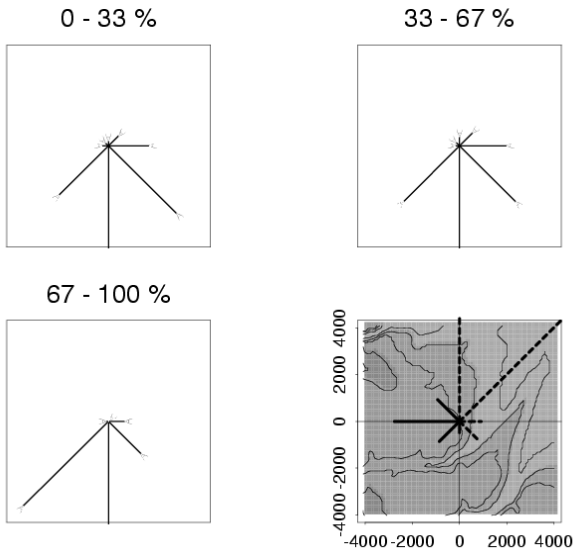

Figure 11. Borden wind roses at 1.5m as a function of the fraction of the buoyant forcing term. Data for 2001. The last panel shows the slope rose, indicating the length of uninterrupted up (solid) or down (dashed) slope in each direction. The horizontal scale is in [m], and the contour spacing is 10 m.

5. SUMMARY AND CONCLUSIONS

In a detailed study of the forest in the immediate area around the flux tower at the Harvard Forest, the canopy structure was shown to be highly variable, both spatially and seasonally. The average canopy profile was bimodal, resulting from the combination of areas of bottom-heavy (coniferous/mixed) and top-heavy (deciduous) foliage distributions. The winter profile was relatively straight, with a resulting wind profile that is well explained by a simple exponential approximation (Cionco, 1985). The more complicated summer profiles require a more sophisticated approach.

Measurements of horizontal obstructions using a laser range finder, and the associated effects of these obstructions on the wind fields, suggested significant inter-seasonal differences, both in directionality and magnitude. The correlation between optically determined obstruction maps and the wind-derived transmission factors was not convincing. This may be improved with a laser system that is either less sensitive to very small obstacles, or has a finer resolution (i.e. a smaller beam width).

The observed canopy structure suggests strong spatial variability in the drag exerted on the flow, as well as the exchange of momentum, energy and trace gases throughout the canopy space, which is commonly treated as a continuous porous medium. However, observations of differences at the various network end points indicated a relatively uniform wind field with only minor flow deflections or attenuations.

Inside the forest, the drag term dominates the momentum equation, especially in summer, with values typically ~ 0.01 m s^{-2} compared to ~ 0.004 m s^{-2} for the stress divergence, buoyancy and pressure gradient terms. While thermal stratification conditions conducive to drainage flows exist in the subcanopy on 92% of all nights, and the buoyancy forcing dominates 58% of the time. As shown in Staebler and Fitzjarrald (2004a), a large fraction of these nights are associated with missing CO_2 fluxes above the canopy, and horizontal transport of CO_2 in the subcanopy.

The pressure gradient term, which was estimated using a linearized theory of flow over hills (Finnigan and Belcher, 2004), did not have any significant diurnal variations on average and accounted for about 30% of the forcing on the subcanopy flows. A Bernoulli speed-up of the wind above the Harvard Forest relative to flat ground was expected due to the local topography. Combining local sodar wind profile measurements with radar profiler measurements 10 km to the WNW suggested a speed-up of 20-60% at heights ~ 150m above ground, compared to ~100% predicted by linear theory.

The stress divergence dominated the daytime flows in the early spring and in the fall, when the canopy was leafless and exposed to seasonally higher synoptic wind speeds. The buoyant term dominated the nights throughout the year, but especially during spring when the ground was still cold and the air above it was warming, creating a stronger surface inversion. Daytime stratification is generally stable inside the forest during the summer, while winter profiles show the effects of solar radiation heating the ground in the absence of foliage.

Subcanopy flows from the northwest significantly increased as the buoyancy term fraction increased, indicating drainage flows from this direction. Both at the

Harvard Forest and at Borden, the deciding factor on the direction of drainage flows appeared to be the length of the slope, not the slope angle. Even at the relatively flat Borden site, drainage flows were shown to be an important feature.

Divergences calculated from a subcanopy array of sonic anemometers often showed a diurnal cycle, suggesting convergence at the Harvard Forest near the ground during daytime hours. However, these divergences could not be reconciled with measured vertical mass flow measurements. These vertical mass flow measurements, at levels of 8 m, 17 m and 29 m above the forest floor, were generally consistent with each other, although the increase of $\overline{w}$ with height appeared to be less than proportional to the height.

There clearly is a need for further measurements to determine why $\overline{w}$ and the divergence are not easily reconciled. The recommended course of action is to measure the divergence at several vertical levels, with towers at the end points of the network, in addition to $\overline{w}$ at these points. It would also be helpful to vary the size of the network, or to have nested arrays, to provide more information on the relevant scales on which local $\overline{w}$ and divergence can be related.

The methodology developed in this work is suited to obtaining a usefully thorough description of both the canopy structure and the wind fields with limited resources. The applicability of the guidelines presented here, such as determining the relevant slopes for drainage flows, should be tested at other sites. Any attempt to establish generally applicable models to describe subcanopy flows will depend on this.

Further model development is needed to describe subcanopy flows, taking into consideration both topography and the canopy density. The goal should be that as more information becomes available on these structural parameters, e.g. from satellite measurements, it will become feasible to use an appropriate model to provide estimates of subcanopy flows, and how these flows may transport scalars such as CO_2, pollutants, pollen and spores.

6. ACKNOWLEDGEMENTS

The authors gratefully acknowledge the assistance of Matt Czikowsky, Sasha Tsoyref, Otávio Acevedo, Kathy Moore, Gary Wojcik, Ricardo Sakai, Jeff Freedman, John Sicker and Dwayne Spiess (ASRC), Bill Munger, John Budney and Steve Wofsy (Harvard University), Geoffrey G. Parker (Smthsonian Environmental Research Center, Edgewater, MD). This research was supported by the Office of Science (BER), U.S. Department of Energy, through the Northeast Regional Center of the National Institute for Global Environmental Change under Cooperative Agreement No. DE-FC02-03ER63613.

7. REFERENCES

Aubinet, M., Heinesch, B., Yernaux, M., 2003: Horizontal and vertical CO_2 advection in a sloping forest. *Bound. Layer Meteorol.* **108**, 397–417.

Aylor, D.E., 1999: Biophysical scaling and the passive dispersal of fungus spores: relationship to integrated pest management strategies. *Agric. Forest Meteorol.,* **97,** 275-292.

Baldocchi, D., et al., 2001: FLUXNET: A new tool to study the temporal and spatial variability of ecosystem-scale carbon dioxide, water vapor, and energy flux densities. *Bulletin Am. Met. Soc.*, **82,** 2415-2434.

Blair, J.B., D.L. Rabine and M.A. Hofton, 1999: The laser vegetation imaging sensor: a medium-altitude, digitization-only, airborne laser altimeter for mapping vegetation and topography. *ISPRS J. Photogramm. Remote Sens.*, **54**, 115-122.

Cionco, R.M., 1985: Modeling windfields and surface layer wind profiles over complex terrain and within vegetative canopies. *In* The Forest-Atmosphere Interaction, Eds. B.A. Hutchison and B.B. Hicks, Reidel Publishing Co., Dordrecht, 684pp.

Finnigan, J.J., 1999: A comment on the paper by Lee (1998): On micrometeorological observations of surface-air exchange over tall vegetation, *Agric. and For. Meteorol.* , **97**, 55-64.

Finnigan, J.J., and S.E. Belcher, 2004: Flow over a hill covered with a plant canopy. *Q. J. Roy. Meteorol. Soc.,* **130,** 1-29.

Fitzjarrald, D.R., 1984: Katabatic wind in opposing flow. *J. Atm. Sc.* , **41,** 1143-1158.

Fitzjarrald, D.R., and K.M. Moore, 1995: Physical mechanisms of heat and mass exchange between forests and the atmosphere. *In: M.Lowman and N. Nadkarni, eds., Forest Canopies: A Review of Research on This Biological Frontier*, Academic Press.

Fitzmaurice, L., R. H. Shaw, K.T. Paw U, and E. G. Patton, 2004: Three-dimensional microfront systems in a large-eddy simulation of vegetation canopy flow. *Bound.-Layer Meteor.* **112**, 107-127.

Fleagle, R.G., 1950: A theory of air drainage. *J. Meteor.*,**7**, 227-232.

Fujita, T.T., and R.M. Wakimoto, 1982: Effects of miso- and mesoscale obstructions on PAM winds obtained during Project NIMROD, *J. Appl. Meteor.,* **21**, 840-858.

Hunt, J.C.R., K.J. Richards and P.W.M. Brighton, 1988: Stably stratified shear flow over low hills. *Q.J.R. Meteorol. Soc.,***114,** 859-886.

Kaimal, J.C., J.E. Gaynor, H.A. Zimmerman, and G.A. Zimmerman, 1990: Minimizing flow distortion errors in a sonic anemometer", *Bound.-Layer Meteorol.*, **53**, 103-115.

Kaimal, J.C., and J.J. Finnigan, 1994: Atmospheric Boundary Layer Flows, Oxford University Press.

Lee, X., 1997: Gravity waves in a forest: a linear analysis. *J. Atmos. Sc.,* **54,** 2574-2585.

Lee, X., 1998: On micrometeorological observations of surface-air exchange over tall vegetation. *Agric. For. Meteorol*., **91**, 39-49.

Lee, X., J.D. Fuentes, R.M. Staebler, and H.H. Neumann, 1999: Long-term Observation of the Atmospheric Exchange of CO_2 with a Temperate Deciduous Forest in Southern Ontario, Canada. *J. Geophys. Res.* **104**, 15975-15984.

Mahrt, L., 1982: Momentum balance of gravity flows. *J. Atmos. Sc*., **39,** 2701-2711.

Mahrt, L., D. Vickers, R. Nakamura, J. Sun, S. Burns, D. Lenschow and M. Soler, 2001: Shallow drainage and gully flows. *Boundary-Layer Meteorol.*, **101**, 243-260.

Moore, K.E., 1987: Nocturnal spore dispersal in young plantations: a micro-meteorological examination of the nighttime surface layer. *Ph.D. Thesis, Dept. of Atm. Science, SUNY Albany.*

Parker, G.G., M.E. Harmon, M.A. Lefsky, J. Chen, R. van Pelt, S.B. Weiss, S.C. Thomas, W.E. Winner, D.C. Shaw and J.F. Franklin, 2004a: Three dimensional structure of an old-growth *Pseudotsuga-Tsuga* canopy and its implications for radiation balance, microclimate, and atmospheric gas exchange. *Accepted, Ecosystems.*

Parker, G.G., D.J. Harding, and M. Berger, 2004b: A portable laser altimeter for rapid determination of forest canopy structure. *Accepted, J. Appl. Ecology.*

Poggi, D., G. G. Katul, and J. D. Albertson, 2004: Momentum transfer and turbulent kinetic energy budgets within a dense model canopy, *Bound-Layer Meteor*. **111**, 589-614.

Prandtl, L., 1942: Führer durch die Ströhmungslehre. Vieweg und Sohn, Braunschweig, 382pp.

Staebler, R.M., J.D. Fuentes, X. Lee, K.J. Puckett, H.H. Neumann, M.J. Deary and J.A. Arnold, 2000: Long term flux measurements at the Borden Forest, *CMOS Bulletin,* **28**, 9-16.

Staebler, R.M., 2003. Forest subcanopy flows and micro-scale advection of carbon dioxide. PhD Dissertation, SUNY Albany.

Staebler, R.M., and D.R. Fitzjarrald, 2004a: Observing subcanopy CO_2 advection. *Agric. Forest Meteorol.,* **122,** 139-156.

Staebler, R.M., and D.R. Fitzjarrald, 2004b: Measuring canopy structure and the kinematics of subcanopy flows in two forests. *Submitted to J. Appl. Met.*

Wilson, K.B., Meyers, T.P., 2001. The spatial variability of energy and carbon dioxide fluxes at the floor of a deciduous forest. *Bound.-Layer Meteorol.*, **98**, 443–473.

Wolfson, M.M., and T.T. Fujita, 1989: Correcting wind speed measurements for site obstructions. *J. Atm.Ocean Tech.,* **6,** 343-352.